



Fluorescence Endoscopy of Cathepsin Activity Discriminates Dysplasia from Colitis

Citation

Gounaris, Elias, John Martin, Yasushige Ishihara, Mohammad Wasim Khan, Goo Lee, Preetika Sinh, Eric Zongming Chen, et al. 2013. "Fluorescence Endoscopy of Cathepsin Activity Discriminates Dysplasia from Colitis." *Inflammatory Bowel Diseases* 19 (7): 1339–45. <https://doi.org/10.1097/mib.0b013e318281f3f8>.

Permanent link

<http://nrs.harvard.edu/urn-3:HUL.InstRepos:41384360>

Terms of Use

This article was downloaded from Harvard University's DASH repository, and is made available under the terms and conditions applicable to Other Posted Material, as set forth at <http://nrs.harvard.edu/urn-3:HUL.InstRepos:dash.current.terms-of-use#LAA>

Share Your Story

The Harvard community has made this article openly available.
Please share how this access benefits you. [Submit a story](#).

[Accessibility](#)



Published in final edited form as:

Inflamm Bowel Dis. 2013 June ; 19(7): 1339–1345. doi:10.1097/MIB.0b013e318281f3f8.

Endoscopic fluorescence imaging of cathepsin activity can discriminate, dysplasia from colitis

Gounaris Elias, PhD¹, Martin John, MD¹, Ishihara Yasushige, MS⁴, Khan Mohammad Wassim, DVM¹, Lee Goo, MD¹, Sinh Preetika, MD¹, Chen Zongming Eric, MD², Michael Angarone, MD³, Ralph Weissleder, MD⁵, Khazaie Khasharyasha, PhD^{1,*}, and Terrence A. Barrett, MD^{1,*}

¹Gastroenterology Division, Feinberg School of Medicine, Northwestern University, Northwestern Memorial Hospital 676 N. St. Clair Street, Suite 1400

²Department of Pathology, Division of Surgical Pathology, Northwestern University Feinberg School of Medicine, 7-340, Feinberg Building 251 E. Huron St. Chicago, IL 60611

³Department of Medicine, Infectious diseases, Northwestern University Feinberg School of Medicine 645 N Michigan Avenue, Suite 900 Chicago IL 60611

⁴Olympus Tokyo, Molecular diagnostic technology Group Advanced Core Technology Department Research and Development Division

⁵Center for Systems Biology, Massachusetts General Hospital and Harvard Medical School, Simches Research Building, 185 Cambridge Street, Boston, Massachusetts 02114, USA

Abstract

BACKGROUND—Surveillance colonoscopy using random biopsies to detect colitis-associated cancer (CAC) suffers from poor sensitivity. Although chromo-endoscopy improves detection, acceptance in the community has been slow. Here, we examine the usefulness of near infrared fluorescence (NIRF) endoscopy to image molecular probes for cathepsin activity in colitis-induced dysplasia.

METHODS—In patient samples, cathepsin activity was correlated with colitis and dysplasia. In mice, cathepsin activity was detected as fluorescent hydrolysis product of substrate based probes (SBPs) after injection into IL-10^{-/-} colitic mice. Fluorescence colonoscopy and colonic whole mount imaging were performed prior to complete sectioning and pathology review of resected colons.

RESULTS—Cathepsin activity was 5 and 8 – fold higher in dysplasia and CAC respectively, compared to areas of mild colitis in patient tissue sections. The signal to noise ratios for dysplastic lesions seen by endoscopy in IL-10^{-/-} mice were 5.2 ±1.3, (P=0.0001). Lesions with increased

*Corresponding Author: Barrett, Terrence, Division of Gastroenterology Northwestern University 676 N. St. Clair, Suite 1400 Chicago, IL 60611 Phone: 312/695-0182 Fax: 312/695-3999, TBarrett@nmff.org. Co-corresponding Author, Khazaie Khasharyasha, Division of Gastroenterology, 303 East Superior Street 3-250 Lurie, Chicago, Illinois 60611-3015, Tel, 312 503 1901 Fax 312 503 0386 khazaie@northwestern.edu.

Contributions: GE designed the project, preformed the experiments, analyzed the data, wrote the paper; KMW, LG, SP, CE, MJ, preformed experiments & analyzed data; IY, designed and developed the fluorescence endoscope; KK, developed the concept and analyzed the data; TAB, Designed the project, analyzed the data, wrote the paper.

NIRF emissions were classified as raised or flat dysplasia, lymphoid tissue and ulcers. Using images collected by endoscopy, a receiver operating characteristic curve (ROC) for correctly diagnosing dysplasia was calculated. The area under the curve was 0.927. At a cut off of 1000 MFI, the sensitivity and specificity for detecting dysplasia were 100% and 83% respectively. Analysis revealed that enhanced NIRF emissions derived from increased numbers of infiltrating myeloid derived suppressor cells and macrophages with equivalent cathepsin activity.

CONCLUSIONS—These studies indicate that cathepsin SBP imaging correctly identifies dysplastic foci within chronically inflamed colons. Cathepsin-based NIRF endoscopy presents unique advantages that may increase sensitivity and specificity of surveillance colonoscopy in patients with CUC.

Keywords

Dysplasia; colitis; macrophages; cathepsin activity; fluorescence endoscopy

Introduction

The relative risk for colorectal cancer (CRC) is high in patients with a history of extensive ulcerative colitis and Crohn's colitis^{1, 2, 3}. For this reason, colitis patients undergo surveillance colonoscopy at regular intervals after eight years of disease⁴. Surveillance examinations increase the detection of CAC at early stages compared to patients not being followed^{5, 6, 7}. In addition, detection of low grade dysplasia (LGD) identifies patients at increased risk for development of high grade dysplasia (HGD) and CRC^{2, 6, 8}. Thus, current surveillance programs improve survival for patients who develop CAC as well as alert physicians to those individuals who require more aggressive surveillance or colectomy.

Surveillance colonoscopy involves taking random biopsies from the colon and sampling or removing suspicious lesions^{9, 10}. The detection of intraepithelial neoplasia (IN) raises concerns that patients have synchronous cancers or progress to HGD or CAC^{11, 12, 13}. Previously, most dysplasia detected microscopically by random biopsies was thought to be "invisible" by white light colonoscopy^{10, 14}. Using modern colonoscopic technologies, Rutter *et al* found that most dysplasia was visible with only 22% detected by random biopsies alone⁹. Dye-enhanced methods increase yields of dysplasia detection 2–3-fold over non-dye-enhanced methods^{2, 8, 14}. In a recent study employing random and dye-enhanced methods, dye-enhanced strategies improved detection 5-fold over random biopsies. Interestingly in 2 of the 102 patients studied, foci of LGD detected by random biopsy methods were not detected by non-dye or dye-enhanced targeted biopsies². Together these findings support the notion that dye-enhanced methods improve sensitivity for LGD detection but raise concerns that some foci may escape detection even by these improved techniques. The clinical relevance of these findings pertain to the potential that early detection of LGD may allow some patients to choose resection and careful follow-up over colectomy¹⁵.

Here we present data that fluorescence imaging of cathepsin activity can be used as a functional indicator of cells that infiltrate into dysplastic lesions. Cathepsins are lysosomal cysteine proteases that contribute to the proteolytic network in tumor microenvironments¹⁶.

Cathepsin activity is localized to subsets of tumor associated macrophages (TAM) and myeloid derived suppressor cells (MDSC). We and others have shown that TAM and MDSC recruitment is increased in colitis¹⁷ and in several tumors including intestinal polyps¹⁸, pancreatic tumors^{19,20} and implanted intra-peritoneal tumors²¹. These findings led to the proposed application of functional imaging to uncovering early dysplasia¹⁸. To detect active cathepsin, mice are injected with a substrate-based probe (SBP) that fluoresces in the near infrared frequency (NIRF) when cleaved. Intact probes fail to emit light due to self-quenching whereas cleavage exposes fluorophores to excitation by NIRF light²². In addition, the strategy for using cathepsin-based probes in the NIRF wavelength allows detection of light emitted at greater tissue depth than reflected white light.

In this article cathepsin activity of the dysplasia infiltrating MDSCs and macrophages were detected by employing fluorescence endoscopy in the colons of *IL-10^{-/-}* mice. We found that cells with cathepsin activity could be detected using a mouse colonoscope modified to image in white light and in NIRF spectrum simultaneously. We observed that NIRF emissions from focal areas of dysplasia were significantly brighter than surrounding areas of colitis. Further studies correlated cathepsin activity with dysplastic pathology in mouse and human colitis tissue. Together the results suggest imaging of cathepsin activity is a sensitive and specific tool for detecting dysplasia in patients with longstanding colitis.

Results

Validation of cathepsin activity emissions in dysplastic lesions using reflectance NIRF imaging

To validate the efficiency of SBPs to detect autochthonous dysplasia over colitis we examined excised colons, previously stained with SBP 680, by reflectance imaging with the reflectance fluorescence device Olympus OV100 device, and calculated the linear NIRF emission profiles of whole colons with Image J software. To correlate the increased emission signal with the relevant histology, colons were Swiss rolled sectioned in 5 μ m sections (~150 sections) and every 10th section was stained with H&E. The sections were examined by pathologists (EC & GL) to determine the type of lesions and distance from the rectum. Examining 3 mice with severe colitis (d28) no dysplasia was detected (Figure 1, A d28 1–3). Areas of moderate increased emission corresponded to focal ulcers (ulcers Vs non-ulcerated inflamed mucosa, mean \pm SEM: 117 \pm 32.45 Vs 78 \pm 19.8 AU, $p < 0.05$) and lymphoid aggregates (lymphoid Vs inflamed, mean \pm SEM: 126 \pm 25.6 Vs 78 \pm 19.8 AU, $p < 0.05$). Differences of emissions between ulcerations and lymphoid aggregates were not statistically significant (Figure 1 B). Colons of d35 mice (n=3) contained ulcers and large lymphoid aggregates with intermediate NIRF emissions (Figure 1, A 35d 1–3).

In one third of the d35 mice examined we observed three high emission peaks that were histologically identified as dysplastic lesions (192.5 \pm 32.6 AU; Figure 1 B). These dysplastic lesions localized to proximal colon, where we normally detect high densities of ulcerated lesions. We speculate that in some cases ulcers and regenerative tissue may be etiologically linked with dysplastic lesions. In six out of nine d56 *IL-10^{-/-}* mice examined, dysplastic lesions with high intensity NIRF emissions were detected. In all nine mice large lymphoid

aggregates were detected in the distal colon with intermediate signal emission (Fig. 1, A 56d 1–3).

By examining all the emission values in aggregate, we found that the mean gray value of dysplastic areas was more than 50% higher than the mean gray value of lymphoid aggregates, 70% higher than ulcers and nearly 2.5-fold higher than microscopic colitis (Fig 1B). All emissions were statistically higher than the emissions from control C57BL/6 mice (n=3) examined indicating inflammation alone increases cathepsin activity. Based on these findings, we conclude that the level of cathepsin activity detected by SBP 680 emission readily discriminates dysplasia from colitis.

The prototype fluorescence endoscope

Having established that NIRF imaging of cathepsin activity discriminates dysplastic lesion on inflamed colitis we collaborated with Olympus Japan in designing and implementing a NIRF fluorescence endoscope. Our aim was to define the condition, under which we could detect dysplastic lesions *in vivo* with a minimally invasive technique.

The excitation light (680 nm, 750 nm) was produced after spectral separation of the white light produced from a Xe lamp. The excitation and the visible light are transmitted through the Olympus BF-XP60 fiberscope into the colon. This fiberscope has a 90° field of view, and a 2–50 mm focal depth. Its outer diameter is 2.8 mm and is uniform throughout its 600 mm length. The fiberscope is equipped with a 1.2 mm instrument channel and has a bending section at the tip (180° up, 130° down). The fluorescent light is collected through a splitter to an emission filter on a high sensitivity CCD camera. The transmitted white light was collected after a splitter to a color CCD camera. The emitted fluorescence and the transmitted white light images were projected on a computer screen and recorded simultaneously with a rate of 10 frames per second (Figure 2). The images collected were converted to time stacks and videos with the use of the NIH Image J software. To calculate the signal to noise ratio (SNR) we select three regions of interest (ROI) 25×25 pixels. One ROI corresponds to the high emissions region, the second is the low emission region, and the third corresponds to the electronic noise of the system. SNR was calculated using the formula (high emissions ROI-electronic noise)/(low emissions-electronic noise). MFI and SNR were recorded using NIH Image J software, and the statistical results were calculated with GraphPad Prism5.

The resolution of the white light camera is not high, a compromise necessary to achieve both wide-angle vision and extended focal depth in this endoscope. With the fluorescence camera, we were able to detect focal increases in emission proven histologically to be colitis-induced dysplasia.

Endoscopic imaging of cathepsin activity SBP identifies dysplastic lesions in colitis

To test the efficacy of cathepsin activity imaging *in vivo*, the prototype endoscopic system was used to detect fluorescent emissions from cathepsin hydrolyzed SBPs in 680nm (Fig. 2). In Fig. 3 are shown representative results of fluorescence endoscopy of *IL-10^{-/-}* mice. *IL-10^{-/-}* mice, injected with SBP 680 (Fig. 3 B) revealed areas of focally increased

emission reflecting elevated cathepsin activity. To determine the histology of tissue areas with high emission, colons were examined *ex vivo* by reflectance fluorescence imaging (Fig. 3 C 1–4). Tissues corresponding to areas of high emission were evaluated histologically. An analysis of the MFI of areas of high emission compared to surrounding non-involved areas permitted calculation of the SNRs. The histopathology of these lesions fell into four categories: type A, dysplastic lesions with raised mucosa (Fig. 3 A3–D 3) associated with high MFI and high SNR (Fig. 3; B, 3 white=MFI and magenta=SNR); type B lesions with flat dysplastic mucosa (Fig. 3 A4–B 4), high MFI and SNR (Fig. 3; B, 4, white=MFI and magenta=SNR), type C lesions with raised mucosa overlying lymphoid tissue (Fig 3; A2–D 2), intermediate MFI and SNR (Fig. 3; B, 2, white=MFI and magenta=SNR) and areas of ulceration also exhibited enhanced cathepsin activity (Fig. 3 A1–D 1), with low to intermediate MFI and SNR (Fig. 3; B, 1, white=MFI and magenta=SNR).

Type A lesions contained raised structures, with numerous dysplastic crypts (Fig. 3; D 3). Type B lesions were flat with microscopic foci of dysplasia containing cells with atypical nuclear morphologies and aberrant crypt structures (Fig. 3; D 4). Type C lesions with intermediate MFI contained large lymphoid aggregates (Fig 3; D 2). Type D lesions contained acute granulation tissue surrounded by reactive/regenerative epithelia (Fig 3; D 1).

To determine the statistical significance of endoscopic NIRF values, the mean fluorescence emission from individual lesions (n=15 mice) were calculated and segregated into groups according to their histology. The mean values associated with both raised and flat dysplastic regions were nearly 2.2-fold higher than those values associated with ulcers or lymphoid aggregates (MFI±SEM: 2049±720 AU for raised dysplasia, 2331±668 AU for flat dysplasia, 939.4±1608 AU for ulcers and 874±408 AU for lymphoid aggregates) and more than 3-fold higher than the microscopically inflamed tissue (647±58.5 AU). One-way ANOVA analysis showed that the MFIs of dysplastic regions were statistically higher than MFIs of non-dysplastic lesions ($P>0.0001$). Non-inflamed colons from C57BL/6 mice had lower cathepsin activity with mean emission 141±26.6 AU (Fig. 3, E). This analysis suggests that MFI values above 1000AU detected all dysplastic lesions. However, the sensitivity for detecting dysplasia dropped as lesions with MFI >1000AU were analyzed. Conversely, the specificity of dysplasia being correctly identified increased progressively for lesions with MFI >1000 (Fig. 5 A&C).

Fluorescence emissions segregates dysplastic from benign lesions

To determine the efficacy of the method of detection we constructed a receiver operating characteristic (ROC) curve using the MFI of raised and flat dysplasia as the test group and the MFI of the lymphoid aggregates, ulcers, and microscopic inflammation as controls. The area under the curve was calculated (Fig. 4). The estimated value of 0.972 confirmed that imaging of cathepsin activity has excellent diagnostic power for discerning dysplasia and cancer from benign tissue inflammation in colitis.

Cathepsin⁺ cells are infiltrating colitis tissue and adenocarcinoma in human colon (CRC)

The efficacy of SBPs to detect cathepsin activity in colitis, sporadic colorectal cancer (CRC) and colitis-associated cancer (CAC) in snap-frozen human biopsy specimens was addressed.

The signal attributed to cathepsin activity was abolished in sections treated with the pan-cathepsin inhibitor, JPM-OEt (Sup. Fig. 1 C 1,2). Results show that compared to un-inflamed controls, 5-fold more cells with cathepsin activity (cathepsin⁺) were present in mild colitis (MLD), 12-fold more in moderate colitis (MOD), 23-fold more in low grade dysplasia (LGD) and 33-fold more in HGD/CAC), compared to normal tissue (Fig. 5). These data indicate that detection of cathepsin activity discriminates dysplastic tissue from benign areas of active colitis in human biopsies.

Discussion

The current study found data to support the clinical testing of fluorescence endoscopy for cathepsin activity in patients with chronic colitis. We propose that imaging of cathepsin activity provides a highly sensitive and specific means for detecting foci of dysplasia within tissue that has ongoing chronic inflammation. Staining for cells with increased cathepsin activity in human tissue sections revealed that areas of LGD and HGD/CAC contained significantly more cathepsin⁺ cells than colitis or normal tissue (Fig. 5 & sup. fig. 1). The increased numbers of cells seen in tissue sections with dysplasia led us to test the practical value of this marker as a tool for detecting dysplasia by endoscopy in mice with colitis-induced dysplasia. Our primary goal was to determine whether imaging of cathepsin activity could detect dysplastic foci within colons with ongoing active inflammation. The results of endoscopic and whole mount tissue imaging indicate that cathepsin activity imaging clearly discriminates dysplasia from surrounding colitis.

Detection of active cathepsins was made possible through use of a novel poly-lysine homopeptide linked with self-quenching Cy 5.5 fluorophores. These probes accumulate within the lysosomes of MDSC and macrophages that infiltrate dysplasia and cancer tissue¹⁸. This feature of SBPs may have increased emissions from dysplastic areas as probes accumulate within cells over the period from injection to imaging 24h later. Thus, live imaging was not reliant on the static assessment of active cathepsin but rather the dynamic activity of cathepsin to hydrolyze probes and accumulate product within areas of dysplasia.

It is possible that areas of early LGD have few surface abnormalities detectable by modern optics or dye-enhanced methods. The current study addresses whether technology directed at alterations in the sub-epithelial layer provide signals for dysplasia. Data in human tissue and live animals suggest that NIRF imaging of a molecular probe for cathepsin activity detects dysplasia in its earliest form. In some cases (Fig 3), LGD was seen in flat lesions indicating that cathepsin imaging delineates dysplastic behavior before surface alterations occur. Thus, detection of functional changes aligned with dysplasia may offer enhanced sensitivity for even invisible forms of LGD.

Analysis of fluorescence emission values from LGD and surrounding flat mucosa indicates that the SNR averages 5:1 over the colitis environment that already has increased cathepsin activity¹⁷(Fig. 5, B). Some variability in SNR was due to differing size and severities of lesions and histology of surrounding mucosa. In areas of LGD surrounded by ulcerated mucosa, the SNR was lower than in regions where LGD occurred amongst mild colitis. In patients undergoing surveillance colonoscopy, LGD may be surrounded by microscopic

colitis¹⁴. Given that dysplastic lesions represent accumulations of MDSC and macrophages within focal lesions, their emission is more concentrated¹⁸. By comparison, cathepsin activity in mild active colitis is more dispersed and therefore less likely to be confused with relatively bright emissions from LGD. One potential area of difficulty may relate to lymphoid tissue. Findings in Fig 3 suggest that NIRF emission from cathepsin activity in raised lymphoid lesions may be confused with raised LGD. Future studies in patients will need to discern how often lymphoid tissue reaches the threshold for targeted biopsies.

We propose that these performance characteristics support the use of a cathepsin-based imaging system in dysplasia detection¹⁸. The potential that NIRF imaging of cathepsin activity will enable detection of colitis-induced dysplasia prior to appearance of endoscopic changes may alter the paradigm of surveillance colonoscopy. It is possible that detection of dysplasia at its earliest stage may allow endoscopists to resect dysplasia at its inception thereby impairing the progression to HGD and cancer.

Supplementary Material

Refer to Web version on PubMed Central for supplementary material.

Acknowledgments

Funding. Northwestern Memorial Hospital, Excellence in Academic Medicine 222 (TAB, EG)

Abbreviations

CAC	Colitis Associated Cancer
MDSC	Myeloid Derived Suppressor Cell
MFI	Mean Fluorescence Intensity
NIRF	Near Infrared Fluorescence
ROC	Receiver Operating Characteristic Curve
SBP	Substrate Based Probe
SNR	Signal to Noise Ratio
TAM	Tumor Associated Macrophages

References

1. Rutter MD, Saunders BP, Wilkinson KH, et al. Cancer surveillance in longstanding ulcerative colitis: endoscopic appearances help predict cancer risk. *Gut*. 2004; 53:1813–1816. [PubMed: 15542520]
2. Marion JF, Wayne JD, Present DH, et al. Chromoendoscopy-targeted biopsies are superior to standard colonoscopic surveillance for detecting dysplasia in inflammatory bowel disease patients: a prospective endoscopic trial. *Am J Gastroenterol*. 2008; 103:2342–2349. [PubMed: 18844620]
3. Ullman TA, Itzkowitz SH. Intestinal inflammation and cancer. *Gastroenterology*. 2011; 140:1807–1816.e1. [PubMed: 21530747]

4. Farraye FA, Odze RD, Eaden J, et al. AGA technical review on the diagnosis and management of colorectal neoplasia in inflammatory bowel disease. *Gastroenterology*. 2010; 138:746–74. 774.e1–4. quiz e12–3. [PubMed: 20141809]
5. Choi PM, Nugent FW, Schoetz DJ, et al. Colonoscopic surveillance reduces mortality from colorectal cancer in ulcerative colitis. *Gastroenterology*. 1993; 105:418–424. [PubMed: 8335197]
6. Ullman TA. Inflammatory bowel disease-associated cancers: does gender change incidence? *Gastroenterology*. 2010; 138:1658–1660. [PubMed: 20332045]
7. Rutter MD, Saunders BP, Wilkinson KH, et al. Thirty-year analysis of a colonoscopic surveillance program for neoplasia in ulcerative colitis. *Gastroenterology*. 2006; 130:1030–1038. [PubMed: 16618396]
8. Rutter MD, Saunders BP, Schofield G, et al. Pancolonic indigo carmine dye spraying for the detection of dysplasia in ulcerative colitis. *Gut*. 2004; 53:256–260. [PubMed: 14724160]
9. Rutter MD, Saunders BP, Wilkinson KH, et al. Most dysplasia in ulcerative colitis is visible at colonoscopy. *Gastrointest Endosc*. 2004; 60:334–339. [PubMed: 15332019]
10. Awais D, Siegel CA, Higgins PDR. Modelling dysplasia detection in ulcerative colitis: clinical implications of surveillance intensity. *Gut*. 2009; 58:1498–1503. [PubMed: 19651634]
11. Ullman T, Lazarev M. Scope early and often in ulcerative colitis and Crohn's colitis? *Gastroenterology*. 2009; 136:718–9. discussion 719–20. [PubMed: 19105962]
12. Connell WR, Lennard-Jones JE, Williams CB, et al. Factors affecting the outcome of endoscopic surveillance for cancer in ulcerative colitis. *Gastroenterology*. 1994; 107:934–944. [PubMed: 7926483]
13. Jess T, Loftus EV, Velayos FS, et al. Incidence and prognosis of colorectal dysplasia in inflammatory bowel disease: a population-based study from Olmsted County, Minnesota. *Inflamm Bowel Dis*. 2006; 12:669–676. [PubMed: 16917220]
14. Kiesslich R, Goetz M, Lammersdorf K, et al. Chromoscopy-guided endomicroscopy increases the diagnostic yield of intraepithelial neoplasia in ulcerative colitis. *Gastroenterology*. 2007; 132:874–882. [PubMed: 17383417]
15. Rutter MD. Surveillance programmes for neoplasia in colitis. *J Gastroenterol*. 2011; 46 (Suppl 1): 1–5. [PubMed: 20798970]
16. Mason SD, Joyce JA. Proteolytic networks in cancer. *Trends Cell Biol*. 2011; 21:228–237. [PubMed: 21232958]
17. Cattaruzza F, Lyo V, Jones E, et al. Cathepsin S is activated during colitis and causes visceral hyperalgesia by a PAR2-dependent mechanism in mice. *Gastroenterology*. 2011; 141:1864–74. e1–3. [PubMed: 21802389]
18. Gounaris E, Tung CH, Restaino C, et al. Live imaging of cysteine-cathepsin activity reveals dynamics of focal inflammation, angiogenesis, and polyp growth. *PLoS ONE*. 2008; 3:e2916. [PubMed: 18698347]
19. Gocheva V, Wang H-W, Gadea BB, et al. IL-4 induces cathepsin protease activity in tumor-associated macrophages to promote cancer growth and invasion. *Genes Dev*. 2010; 24:241–255. [PubMed: 20080943]
20. DeNardo DG, Johansson M, Coussens LM. Immune cells as mediators of solid tumor metastasis. *Cancer Metastasis Rev*. 2008; 27:11–18. [PubMed: 18066650]
21. Youn J-I, Gabrilovich DI. The biology of myeloid-derived suppressor cells: the blessing and the curse of morphological and functional heterogeneity. *Eur J Immunol*. 2010; 40:2969–2975. [PubMed: 21061430]
22. Weissleder R, Tung CH, Mahmood U, et al. In vivo imaging of tumors with protease-activated near-infrared fluorescent probes. *Nat Biotechnol*. 1999; 17:375–378. [PubMed: 10207887]

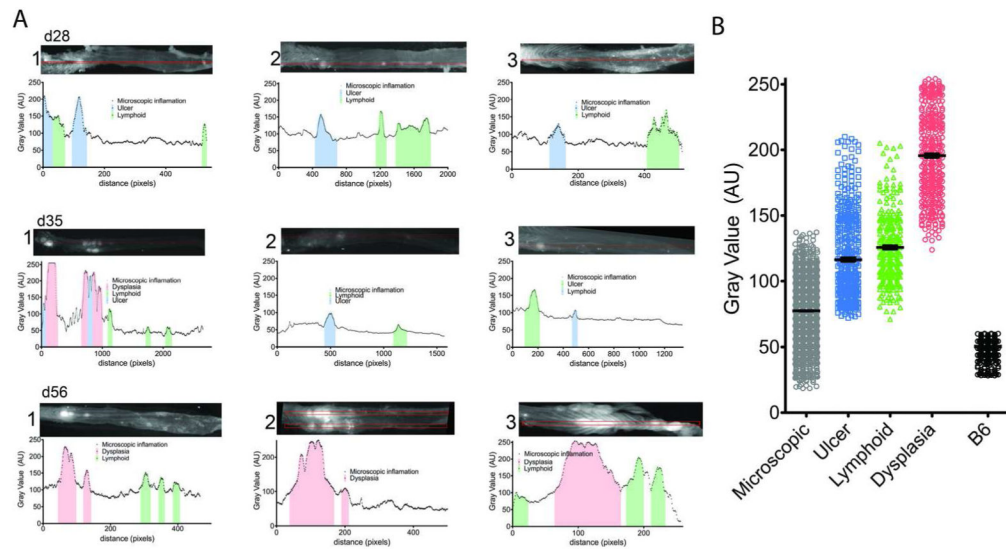


Figure 1. Emission patterns of colitis lesions in representative mice

A) Representative patterns of three colons each from d28, d35 and d56 mice are shown. The patterns represent the emission values per pixel alongside a box 5 pixels x the length of the colon. The color shaded areas of the graphs represent verified areas of ulcers (blue), lymphoid aggregates (green) and dysplasia (red). On the top of each graph are the reflectance fluorescence images of each colon analyzed. (B) Cumulative plots of the emission values of each type of lesions analyzed: microscopic (gray), ulcer (blue), lymphoid aggregates (green), dysplastic lesions (red) and healthy B6 colon (black) are shown.

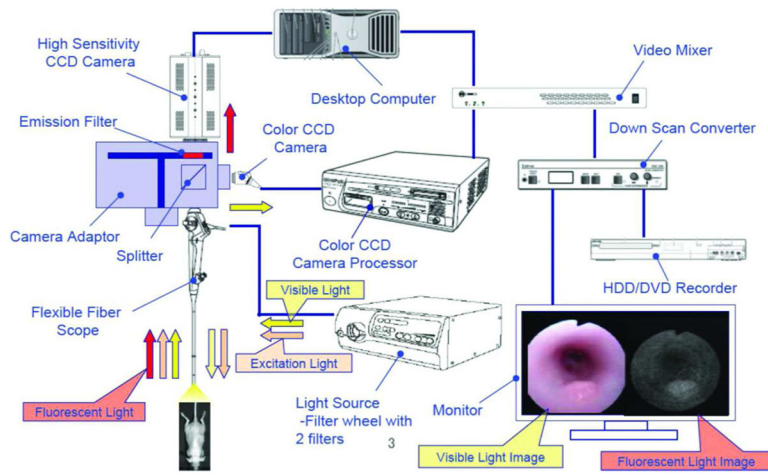


Figure 2.
Diagram of the small animal fluorescence endoscope as designed by Olympus.

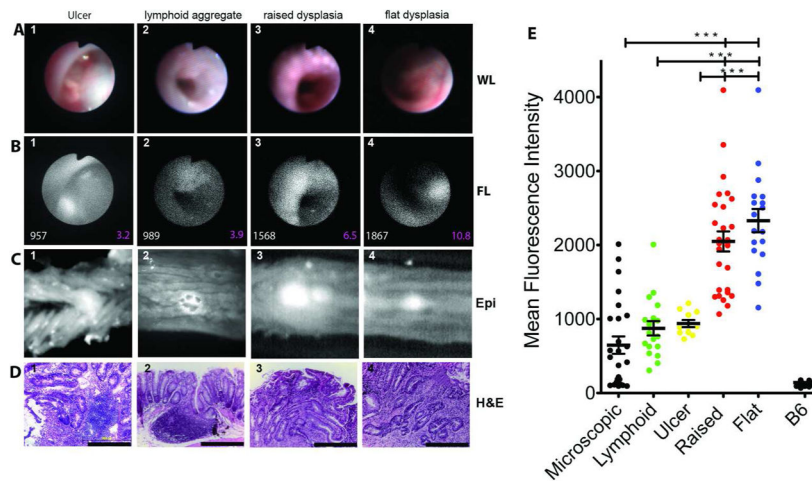


Figure 3. Focal increases of cathepsin activity emission designate dysplastic lesions in *IL10*^{-/-} mice with active colitis

(A) White light endoscopic images of lesions that correspond to (B) representative areas of focally increased NIRF emission of cathepsin activity mouse colon MFI of the lesions are shown in white fonts and SNR in magenta. In (C) is shown reflectance fluorescence image of the lesions extracted from whole mounts colon examined in A and B (660nm). (D) H&E images (x400) of the representative lesions shown in (A) & (B). (E) Cumulative plot of MFI of the lesions observed in the 15 mice examined.

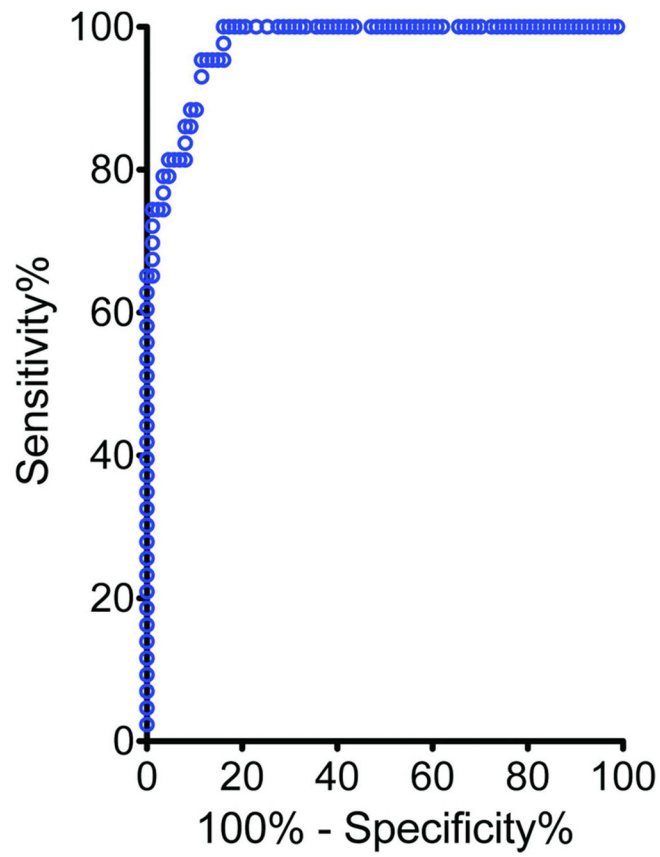


Figure 4.
OC curve testing the sensitivity and specificity in detecting raised and flat lesions over colitis associated structures

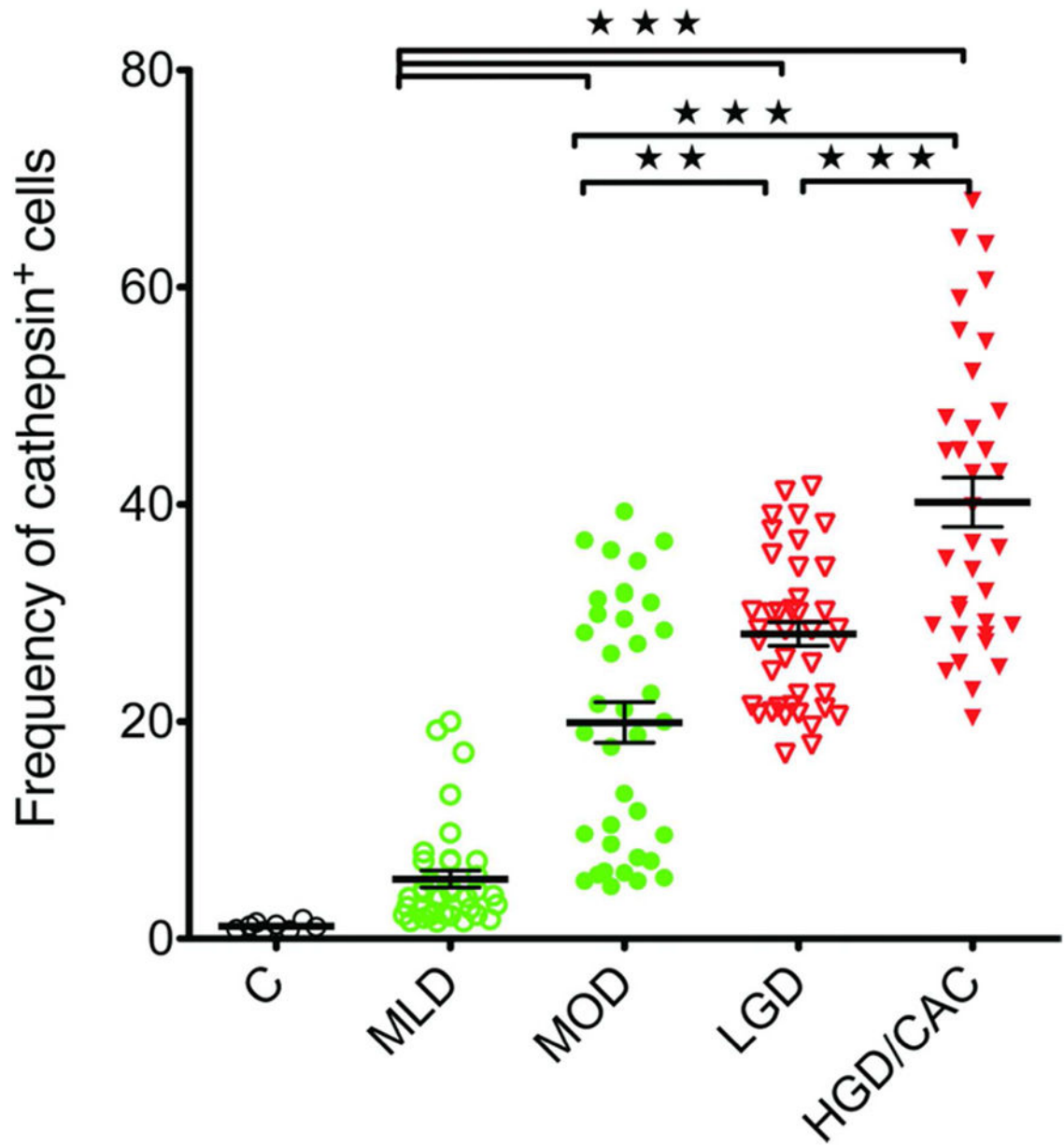


Figure 5. Numbers of cathepsin+ cells are increased in areas of dysplasia compared to colitis in patient biopsies: Dot plot frequencies of cathepsin+ cells stratified according to H&E analysis. Control (C), mild colitis (MLD), moderate colitis (MOD), low-grade dysplasia (LGD) and high grade dysplasia and colitis-associated cancer (HGD/CAC)

Table 1

Types of lesions with high to moderate emissions.

	Mucosa	MFI	SNR	Histology
Type A	Raised	High	High	Dysplastic
Type B	Flat	High	High	Dysplastic
Type C	Raised	Moderate	Moderate	Lymphoid aggregate
Type D	Raised	Moderate	Moderate	Ulcer